Supporting Information for

Highly flexible, mesoporous structured, and metallic Cu-doped C/SiO_2 nanofibrous membranes for efficient catalytic oxidative elimination of antibiotic pollutants

Haoru Shan,[ac] Xiangyang Dong,[b] Xiaota Cheng,[ac] Yang Si,*[ac] Jianyong Yu,*[c] and Bin Ding[ac]

[a] State Key Laboratory for Modification of Chemical Fibers and Polymer Materials, College of Textiles, Donghua University, Shanghai 201620, China

[b] School of Resource and Environmental Science, Wuhan University, Wuhan 430079, China

[c] Innovation Center for Textile Science and Technology, Donghua University, Shanghai 200051, China

* Corresponding authors:

E-mail address: yangsi@dhu.edu.cn (Prof. Y. Si); yujy@dhu.edu.cn (Prof. J. Yu)

Supplementary Methods

Fractal Dimension Calculation

The fractal dimension (D) was calculated from the corresponding N_2 adsorption isotherms according to the following Frenkel-Halsey-Hill (FHH) equation:

$$\ln(V/V_{mono}) = A\left[\ln\left(\ln\left(P_0/P\right)\right)\right] + C \tag{1}$$

where V is N_2 adsorption capacity at each equilibrium pressure; V_{mono} is the monolayer adsorption capacity; P_0 and P are the saturation and equilibrium pressure, respectively; and plots of $\ln(V/V_{\mathrm{mono}})$ versus $\ln(\ln(P_0/P))$ showing a linear trend were reconstructed and the D could be calculated by utilizing the expression: $D = A + 3$, which was according to the dominant forces of liquid-gas surface tension at high coverage.

Apparent Rate Constants Determination

The pseudo-first-order (eqn (2)) and second-order (eqn (3)) kinetic models are described in the following way:

$$\ln\frac{C_t}{C_0} = -k_{obs}t \tag{2}$$

$$\frac{1}{C_t} - \frac{1}{C_0} = kt \tag{3}$$

where C_0 (mg L^{-1}) is the initial concentration of TCH, C_t (mg L^{-1}) is the residual concentration of TCH at t (min), and k_{obs} (min^{-1}) is the reaction rate constant of the pseudo-first-order model, respectively; k (L mg^{-1} min^{-1}) is the rate constant of a second-order reaction.

Activation Energy Calculation

The correlation between the rate constants and reaction temperature was fitted by the Arrhenius equation (eqn(4)).

$$\ln k = \ln A - \frac{E_a}{RT} \tag{4}$$

where k is rate constant of pseudo-second-order reaction (L mg^{-1} min^{-1}), A is the pre-exponential factor, E_a (kJ mol^{-1}) is the Arrhenius activation energy or apparent activation energy, R is molar gas constant of 8.814472×10^{-3} kJ mol^{-1} K^{-1}, and T is the reaction temperature (K).

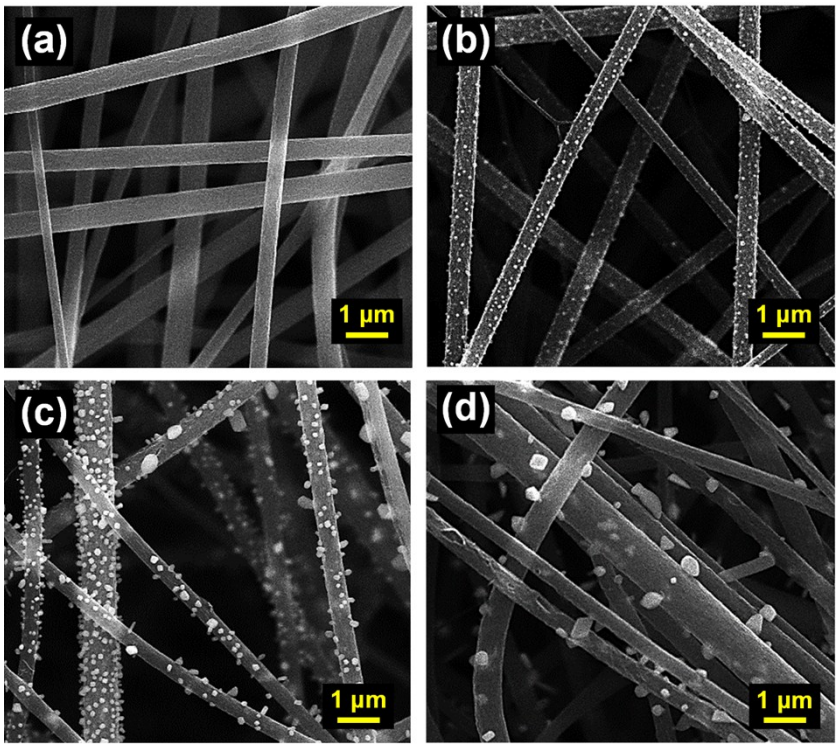

Fig. S1. SEM images of (a) Cu@C/SiO_2-1 NFMs, (b) Cu@C/SiO_2-2 NFMs, (c) Cu@C/SiO_2-3 NFMs, and (d) Cu@C/SiO_2-4 NFMs.

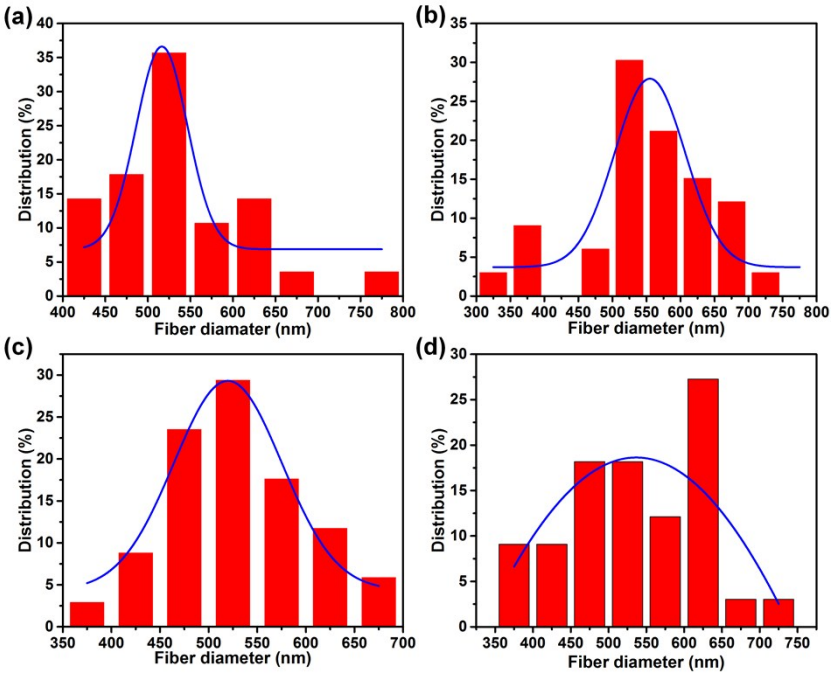

Fig. S2. Histograms of fiber diameter distribution for (a) Cu@C/SiO_2-1 NFMs, (b) Cu@C/SiO_2-2 NFMs, (c) Cu@C/SiO_2-3 NFMs, and (d) Cu@C/SiO_2-4 NFMs.

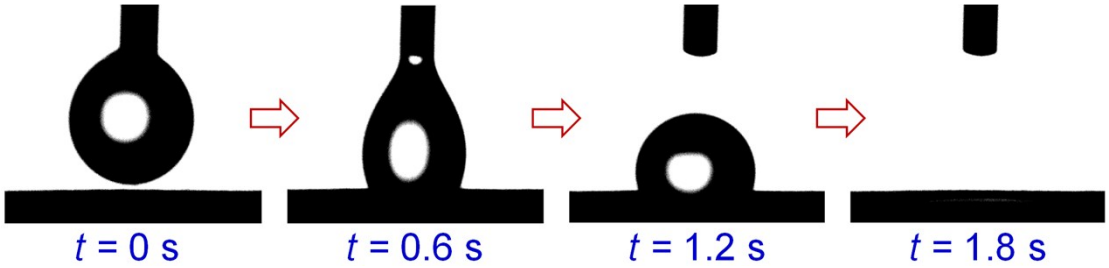

Fig. S3. Photographs of dynamic measurements of water permeation on the Cu@C/SiO_2-3 NFMs.

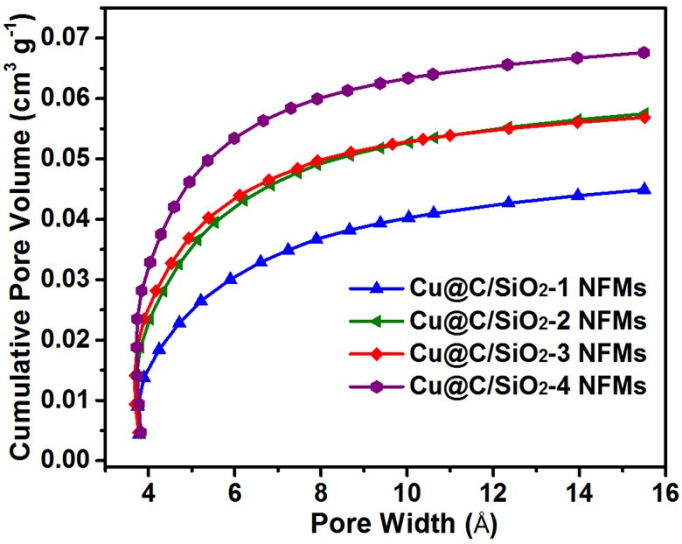

Fig. S4. Horvath-Kawazoe cumulative pore volume plots of the relevant Cu@C/SiO_2 NFMs.

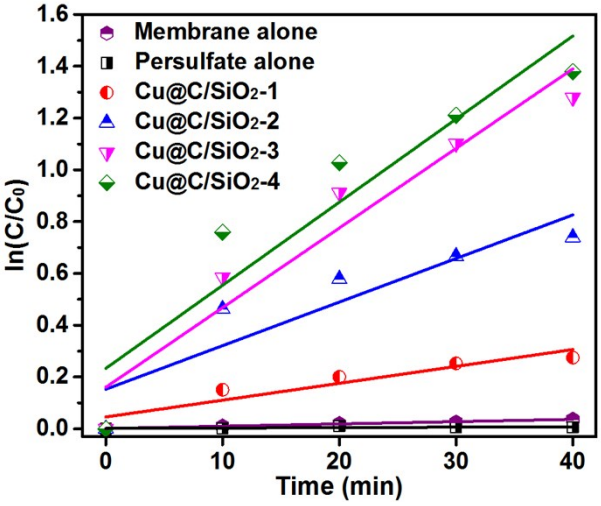

Fig. S5. Pseudo-first-order kinetic plots of the relevant Cu@C/SiO_2 NFMs.

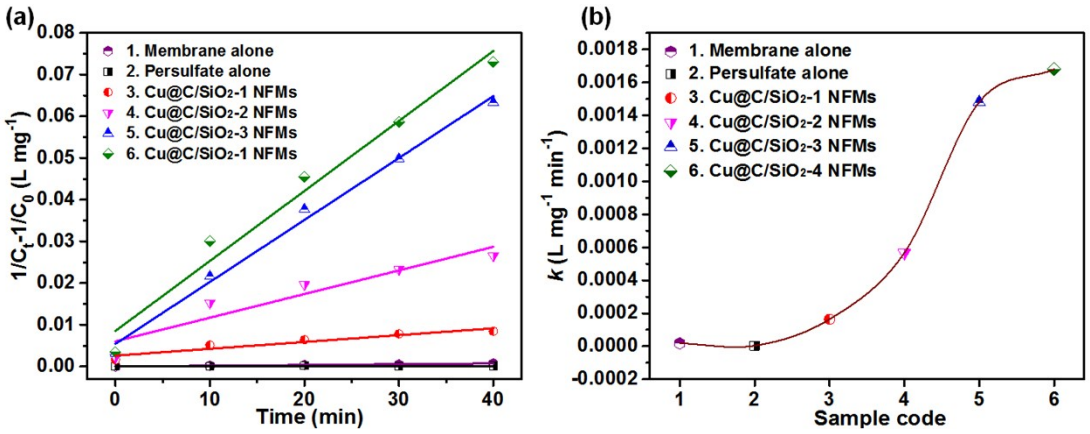

Fig. S6. (a) Pseudo-second-order kinetic plots of the relevant Cu@C/SiO_2 NFMs. (b) The calculated rate constant of Pseudo-second-order kinetics.

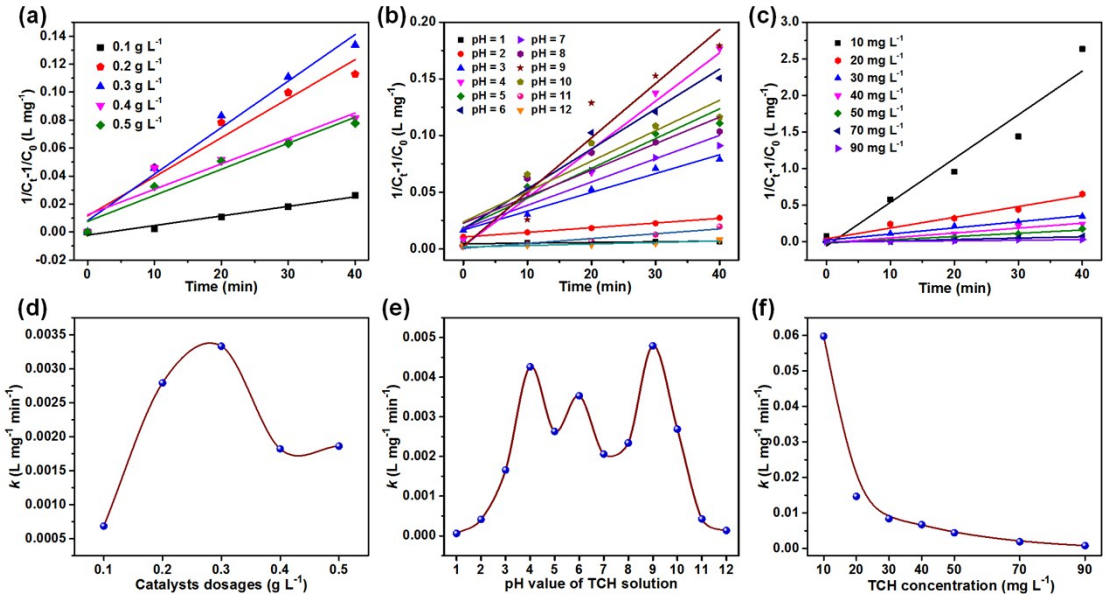

Fig. S7. The pseudo-second-order kinetics for catalyst at various reaction parameters: (a) catalyst dosages, (b) pH values, and (c) TCH concentrations. (d-f) The degradation rates for the corresponding reaction parameters.

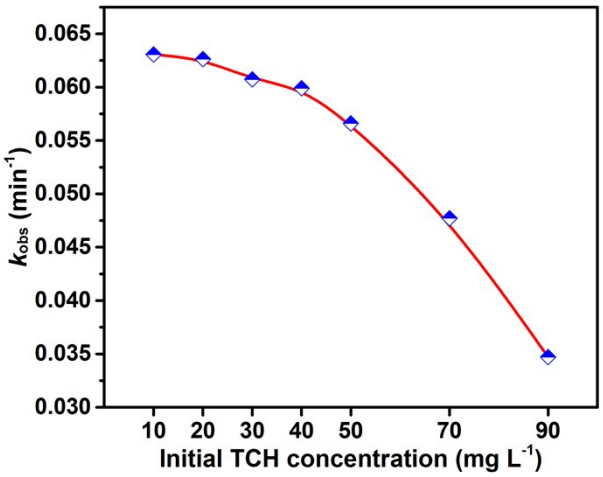

Fig. S8. Effect of initial concentration of TCH aqueous solution on degradation rate.

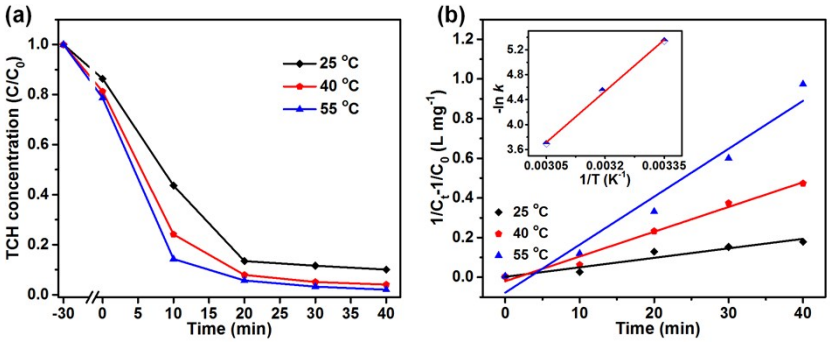

Fig. S9. (a) Effect of reaction temperature on TCH degradation. (b) $1/C_t$-$1/C_0$ versus reaction time based on the effect of reaction temperature. Inset indicates the Arrhenius curve. Reaction conditions: [Catalyst dosages] = 0.3 g L^{-1}, [persulfate dosages] = 0.3 g L^{-1}, [pH value] = 9, [TCH concentration] =50 mg L^{-1}.

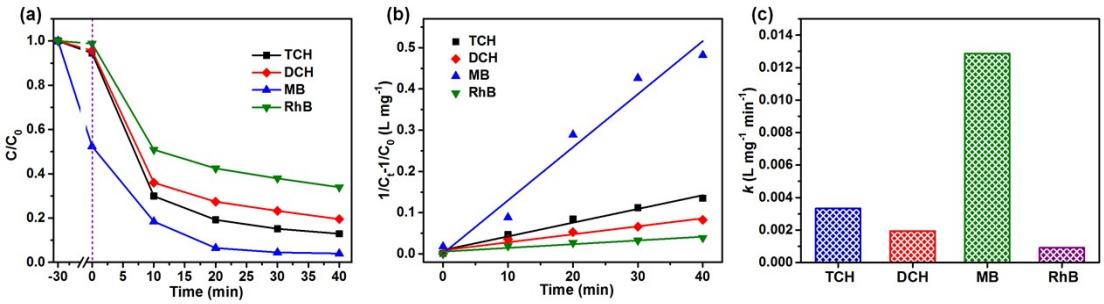

Fig. S10. (a) Oxidation degradation properties of TCH, DCH, MB, and RhB through Cu@C/SiO_2 NFMs-persulfate system. (b) The corresponding pseudo-second-order kinetic plots. (c) The degradation rate for TCH, DCH, MB, and RhB.

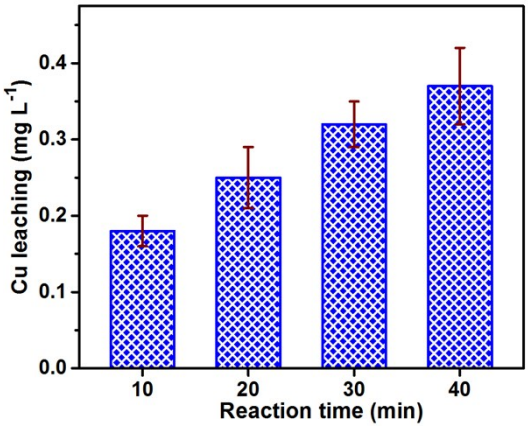

Fig. S11. Cu leaching during the reaction in the Cu@C/SiO_2 NFMs-persulfate system. Reaction conditions: [Cu@C/SiO_2 NFMs] = 0.3 g L^{-1}, [persulfate] = 0.3 g L^{-1}, pH = 7.

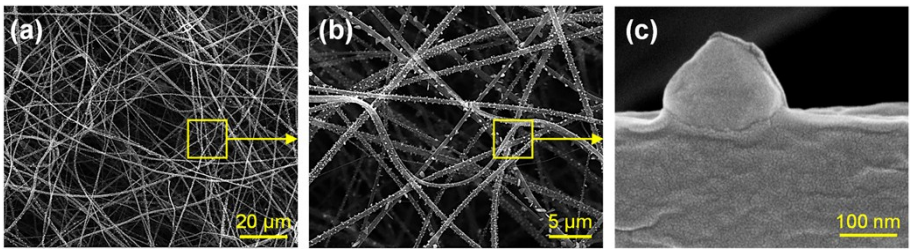

Fig. S12. (a-c) SEM images of Cu@C/SiO_2-3 NFMs after continuous degradation processes at gradually increased magnifications.

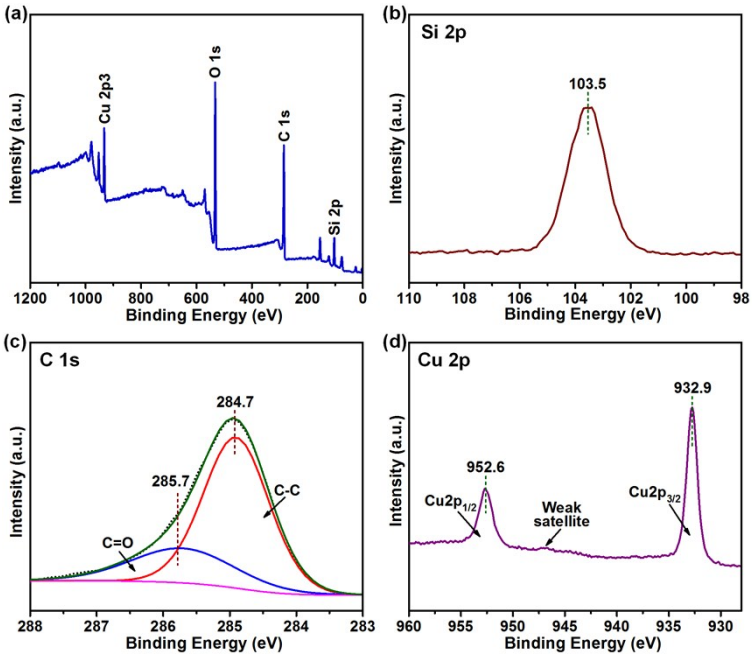

Fig. S13. XPS analysis of the Cu@C/SiO_2-3 NFMs after use, (a) XPS survey, (b) Si 2p, (c) C 1s, and (d) Cu 2p spectra.

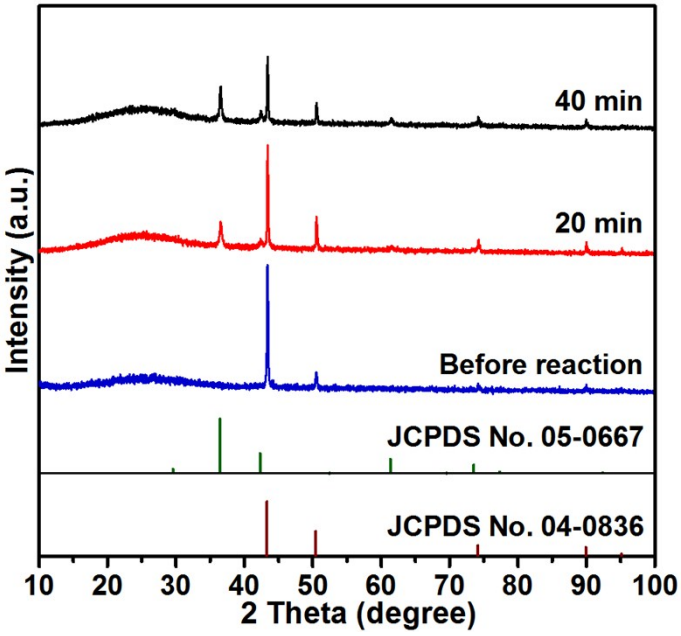

Fig. S14. XRD patterns of Cu@C/SiO_2-3 NFMs before and after reaction.

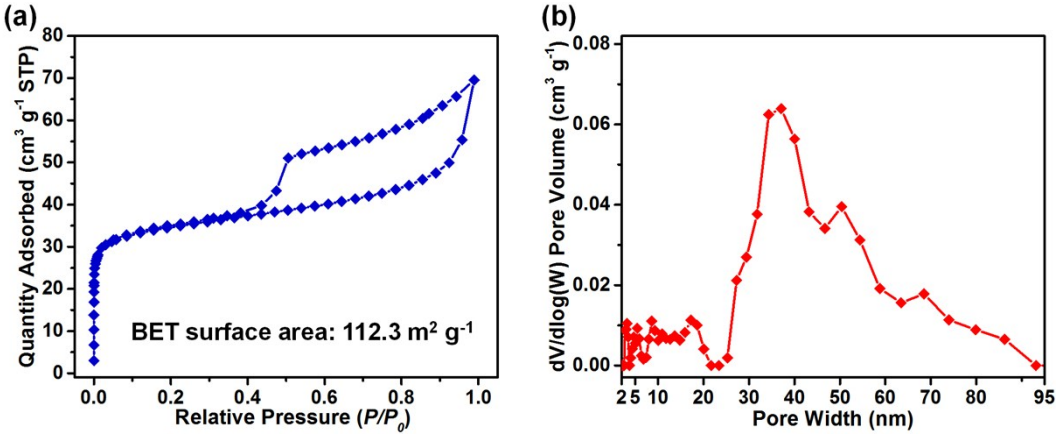

Fig. S15. (a) Nitrogen adsorption-desorption isotherms and (b) pore size distribution curves of Cu@C/SiO_2-3 NFMs after degradation processes.

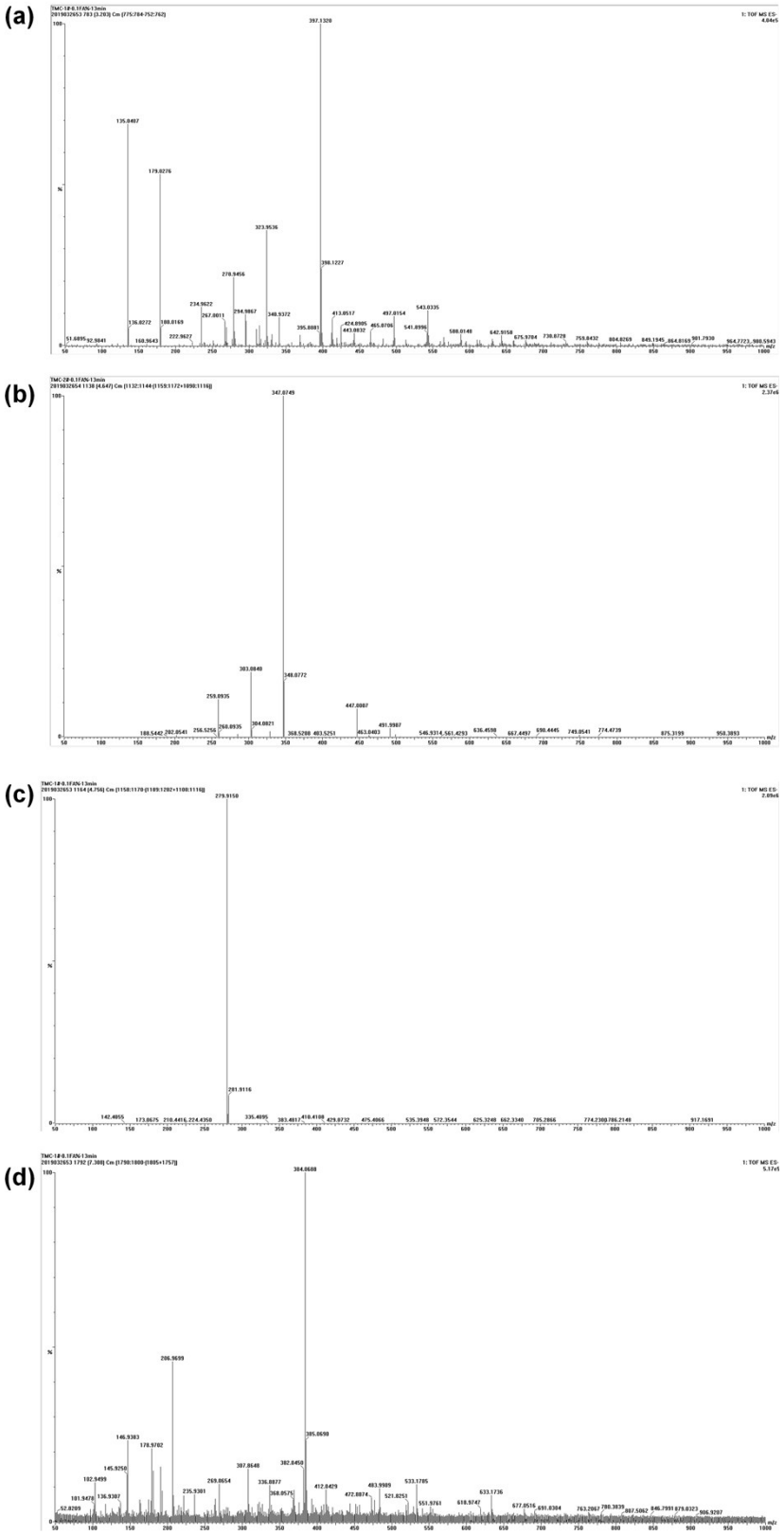

Fig. S16. UPLC-MS spectra of the residual TCH solution during catalyzed *via* Cu@C/SiO_2-3 NFMs/persulfate system.

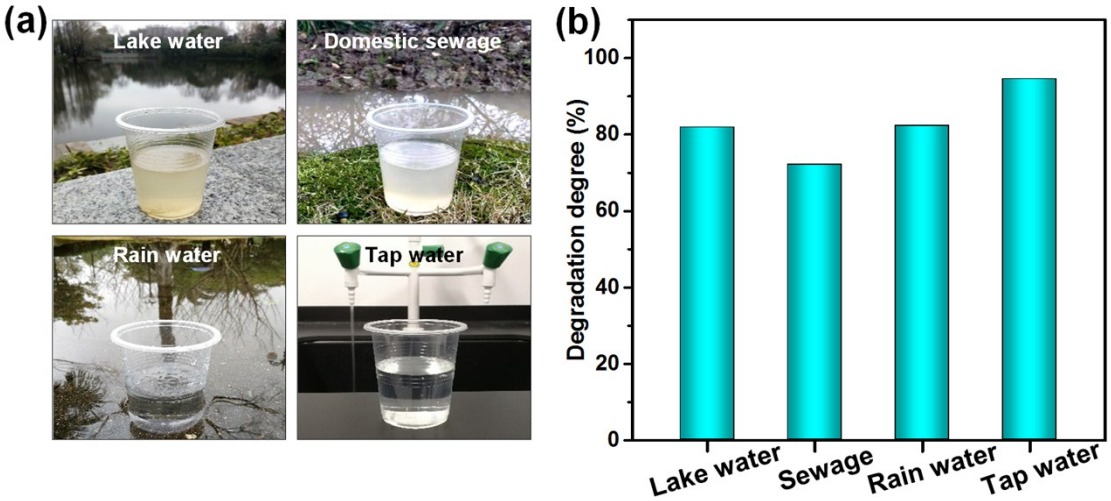

Fig. S17. (a) Natural water samples obtained from lake water, domestic sewage, rainwater, and tap water, respectively. (b) The corresponding TCH degradation performance based on the natural water samples.

Table S1. Porous structural parameters of the relevant Cu@C/SiO_2 NFMs.

Sample name	S_{BET}[a] (m^2 g^{-1})	V_{total}[b] (cm^3 g^{-1})	V_{meso}[c] (cm^3 g^{-1})	V_{micro}[d] (cm^3 g^{-1})	PVF_{meso}[e] (%)
Cu@C/SiO_2-1 NFMs	94.56	0.164	0.119	0.045	72.6
Cu@C/SiO_2-2 NFMs	115.87	0.146	0.089	0.057	61.0
Cu@C/SiO_2-3 NFMs	118.66	0.143	0.086	0.057	60.1
Cu@C/SiO_2-4 NFMs	133.64	0.157	0.090	0.067	57.3

[a]Specific surface area was calculated *via* BET method. [b]Total pore volume was calculated at P/P0= 0.99. [c]*V*meso was calculated through NLDFT model. [d]*V*micro was calculated through HK model. [e]PVF_{meso} indicates the pore volume fraction of mesopores.

Table S2. Degradation kinetics parameters for for various Cu@C/SiO_2 NFMs.

Sample name	**Pseudo-first-order model**		**Pseudo-second-order model**	
	k_{obs} (min^{-1})	R^2	k (L mg^{-1} min^{-1})	R^2
1. Membrane alone	0.00089	0.961	0.00002	0.988
2. Persulfate alone	0.00015	0.937	0.00003	0.958
3. Cu@C/SiO_2-1 NFMs	0.0071	0.925	0.00016	0.952
4. Cu@C/SiO_2-2 NFMs	0.01706	0.924	0.00056	0.957
5. Cu@C/SiO_2-3 NFMs	0.03121	0.934	0.00148	0.991
6. Cu@C/SiO_2-4 NFMs	0.03235	0.916	0.00168	0.969

Table S3. Degradation kinetics parameters for different catalyst dosages.

Catalysts dosages ($g\ L^{-1}$)	Pseudo-first-order model		Pseudo-second-order model	
	k_{obs} (min^{-1})	R^2	k ($L\ mg^{-1}\ min^{-1}$)	R^2
0.1	0.02179	0.978	0.00068	0.987
0.2	0.04286	0.747	0.00279	0.931
0.3	0.04661	0.800	0.00333	0.974
0.4	0.03403	0.666	0.00182	0.852
0.5	0.03557	0.781	0.00186	0.943

Table S4. Degradation kinetics parameters for different pH values.

pH value	Pseudo-first-order model		Pseudo-second-order model	
	k_{obs} (min^{-1})	R^2	k ($L\ mg^{-1}\ min^{-1}$)	R^2
1	0.00234	0.906	0.00006	0.915
2	0.01079	0.909	0.00041	0.997
3	0.02597	0.942	0.00166	0.975
4	0.04747	0.927	0.00426	0.962
5	0.03979	0.689	0.00263	0.923
6	0.04558	0.727	0.00353	0.937
7	0.03538	0.648	0.00206	0.934
8	0.03736	0.602	0.00234	0.915
9	0.05395	0.956	0.00479	0.958
10	0.03935	0.630	0.00269	0.921
11	0.01423	0.902	0.00042	0.913
12	0.00542	0.861	0.00013	0.934

Table S5. Degradation kinetics parameters for different TCH concentrations.

TCH concentration ($mg\ L^{-1}$)	Pseudo-first-order model		Pseudo-second-order model	
	k_{obs} (min^{-1})	R^2	k ($L\ mg^{-1}\ min^{-1}$)	R^2
10	0.06306	0.903	0.05978	0.919
20	0.06264	0.783	0.01467	0.965
30	0.06073	0.803	0.00843	0.983
40	0.05991	0.926	0.00672	0.937
50	0.05395	0.956	0.00479	0.958
70	0.04772	0.902	0.00191	0.933
90	0.03471	0.889	0.00080	0.929

Table S6. Kinetic rate constants and activation energies of TCH degradation.

T (°C)	k (L mg^{-1} min^{-1})	R^2	ΔE (kJ mol^{-1})
25	0.00479	0.903	47.7
40	0.01248	0.977	/
55	0.02418	0.948	/

Table S7. Characteristic parameters of the representative antibiotic molecules.

Antibiotics type	Chemical structure	Molecular size	Molecular volume (nm^3)
Tetracycline hydrochloride (TCH)	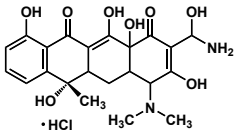	1.41 nm × 0.46 nm × 0.82 nm	0.532
Doxycycline hydrochloride (DCH)	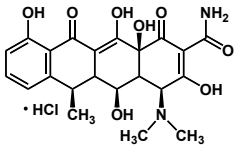	1.41 nm × 0.45 nm × 0.85 nm	0.539
Methylene Blue (MB)	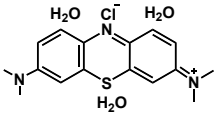	1.43 nm× 0.61 nm × 0.4 nm	0.349
Rhodamine B (RhB)	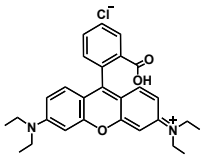	1.59 nm× 1.18 nm × 0.56 nm	1.051

Table S8. Degradation performance of Cu@C/SiO_2 NFMs towards TCH in comparison with state of art catalysts in literatures.

Catalyst	Reaction rate (min^{-1})	Removal ability	Reaction conditions	Ref.
Cu@C/SiO_2 NFMs	0.054	95% within 40 min	[Catalyst] = 0.3 g L^{-1}, [persulfate] = 0.3 g L^{-1}, [TCH] = 50 mg L^{-1}	This work
Cu-FeOOH/BC	0.0178	98% within 180 min	[Catalyst] = 0.2 g L^{-1}, [persulfate] = 20 mM, [TCH] = 20 mg L^{-1}	[1]
Cu/$CuFe_2O_4$	/	68.3% within 120 min	[Catalyst] = 0.3 g L^{-1}, [persulfate] = 1.5 g L^{-1}, [TCH] = 50 mg L^{-1}	[2]
Activated carbon/Fe_3O_4	0.0058	99.9% within 180 min	[Catalyst] = 0.2 g L^{-1}, [persulfate] = 30 mM, [TCH] = 50 mg L^{-1}	[3]
$Ni_xFe_{3-x}O_4$	0.038	85% within 35 min	[Catalyst] = 0.35 g L^{-1}, [persulfate] = 42 μM, [TCH] = 20 mg L^{-1}	[4]
Fe/C	0.218	92.1% within 12 min	[Catalyst] = 0.2 g L^{-1}, [persulfate] = 5 g L^{-1}, [TCH] = 100 mg L^{-1}	[5]
Co/$BiFeO_3$	/	81.09% within 60 min	[Catalyst] = 0.5 g L^{-1}, [persulfate] = 3.33 g L^{-1}, [TCH] = 10 mg L^{-1}	[6]

Reference

1. J. Xu, X. Zhang, C. Sun, J. Wan, H. He, F. Wang, Y. Dai, S. Yang, Y. Lin, X. Zhan, *Environ. Sci. Pollut. Res.*, 2019, **26**, 2820-2834.
2. Z. Li, C. Guo, J. Lyu, Z. Hu, M. Ge, *J. Hazard. Mater.*, 2019, **373**, 85-96.
3. A. Jafari, B. Kakavandi, N. Jaafarzadeh, R. Kalantary, M. Ahmadi, A. Babaei, *J. Ind. Eng. Chem.*, 2017, **45**, 323-333.
4. R. Guan, X. Yuan, Z. Wu, H. Wang, L. Jiang, J. Zhang, Y. Li, G. Zeng, D. Mo, *Chem. Eng. J.*, 2018, **350**, 573-584.
5. X. Jiang, Y. Guo, L. Zhang, W. Jiang, R. Xie, *Chem. Eng. J.*, 2018, **341**, 392-401.
6. H. Zhang, S. Cheng, B. Li, X. Cheng, Q. Cheng, *Sep. Purif. Technol.*, 2018, **202**, 242-247.